Supplementary materials

Effects of partial attachment at the interface between receptor and substrate on nanomechanical cantilever sensing

Kosuke Minami,[a,b,*] Genki Yoshikawa[b,c]

[a] *International Center for Young Scientists (ICYS), National Institute for Materials Science (NIMS), 1-1 Namiki, Tsukuba, Ibaraki 305-0044, Japan*

[b] *Center for Functional Sensor & Actuator (CFSN), National Institute for Materials Science (NIMS), 1-1 Namiki, Tsukuba, Ibaraki 305-0044, Japan*

[c] *Materials Science and Engineering, Graduate School of Pure and Applied Science, University of Tsukuba, 1-1-1 Tennodai, Tsukuba, Ibaraki 305-8571, Japan.*

* *To whom correspondence should be addressed. E-mail: MINAMI.Kosuke@nims.go.jp (K. M.)*

Contents

Supplementary Notes

Note S1. Condition of finite element analysis of width-dependency

To construct the interfacial structure with the width of the coating film, $w_f = 2$ [μm], the mesh was not able to be constructed by COMSOL Multiphysics® 5.4. Therefore, the width of the coating film for the interfacial structure with $w_f = 2.9$ [μm] instead of $w_f = 2$ [μm] was calculated.

Note S2. Generation of random number using Python with numpy module

To investigate the effects of interfacial attachments for realistic or practical conditions, the pillar-like structures were placed at the randomly distributed model according to the random number generated by Python with numpy module. The script is shown in below and detailed numbers are shown in Table S3.

```
import numpy as np
np.random.seed(1)
rn1 = np.random.rand(100,2)

np.random.seed(2)
rn2 = np.random.rand(100,2)

np.random.seed(3)
rn3 = np.random.rand(100,2)

np.random.seed(4)
rn4 = np.random.rand(100,2)

np.random.seed(5)
rn5 = np.random.rand(100,2)
```

Supplementary Figures

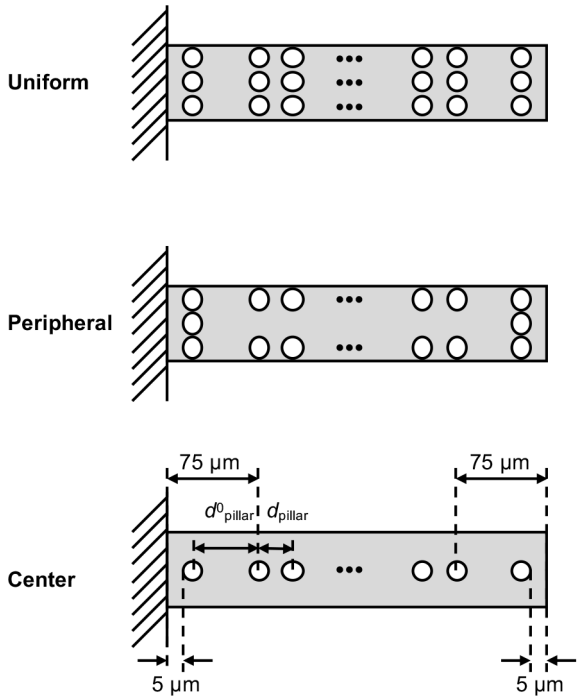

Fig. S1. Detailed configuration of the interfacial attachment models.

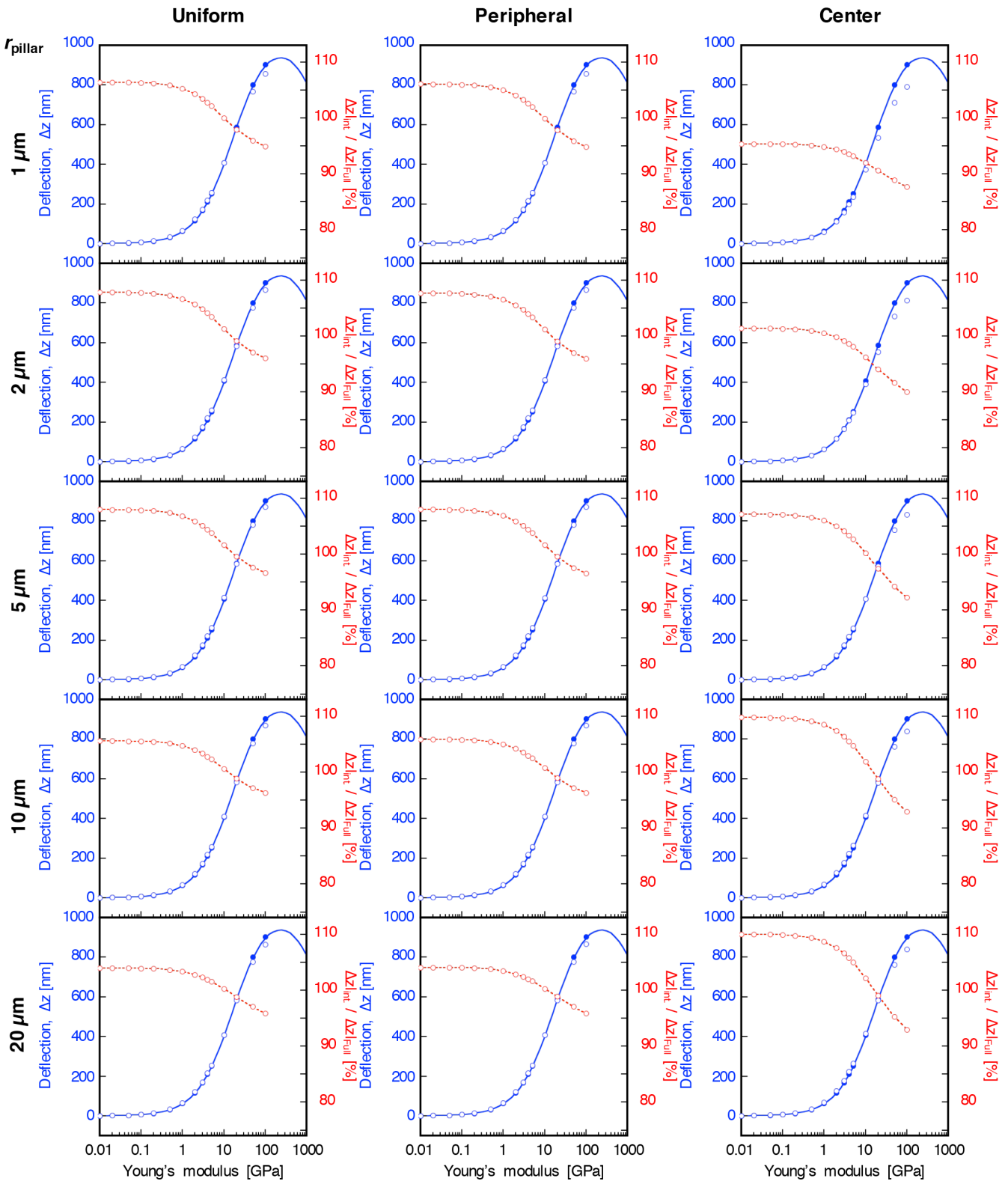

Fig. S2. Detailed effects of interfacial attachment models. Deflections of a free end of a cantilever, Δz as a function of Young's modulus of the coating film, E_f, as presented in Fig. 2b in the main text. Blue lines and blue solid circles indicate the deflections of the fully attached models, $\Delta z|_{Full}$ calculated by analytical solutions from Eq. (2) and numerical solutions using FEA, respectively, and blue open circles indicate the deflections of the interfacial attachment models, $\Delta z|_{int.}$ simulated by FEA. Red open circles are relative deflections of interfacial attachment models, $\Delta z|_{int.} / \Delta z|_{Full}$ [%].

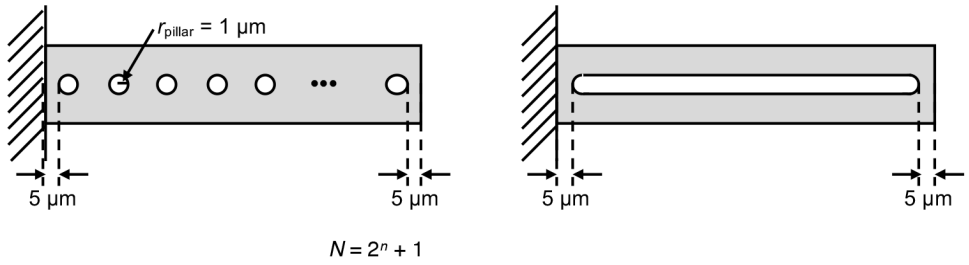

Fig. S3. Configuration of the distance-dependent center aligned models (*left*) and connected model (*right*).

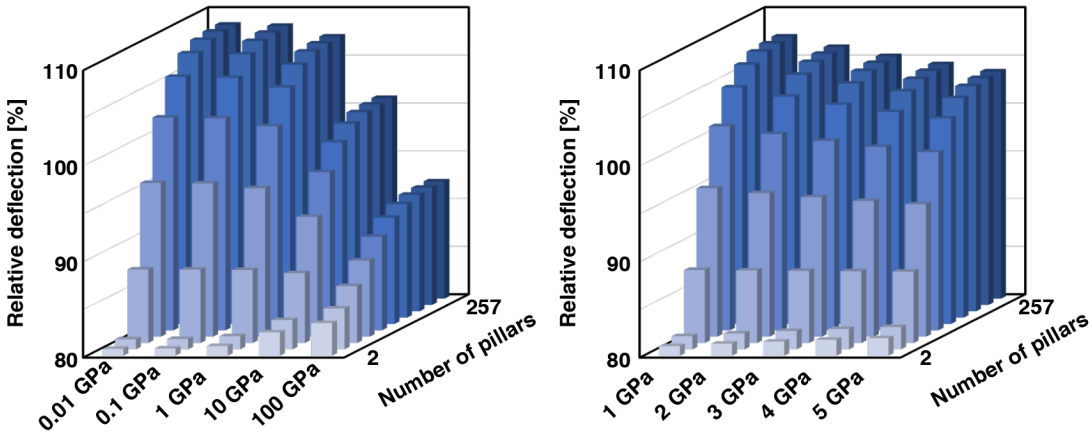

Fig. S4. Relative deflections of center aligned model compared with the fully attached model. Results of the FEA simulations for center aligned model with different number of pillars. Δz_{int} / Δz_{full} [%], where Δz_{int} and Δz_{full} are the deflections of interfacial models and fully attached models, respectively.

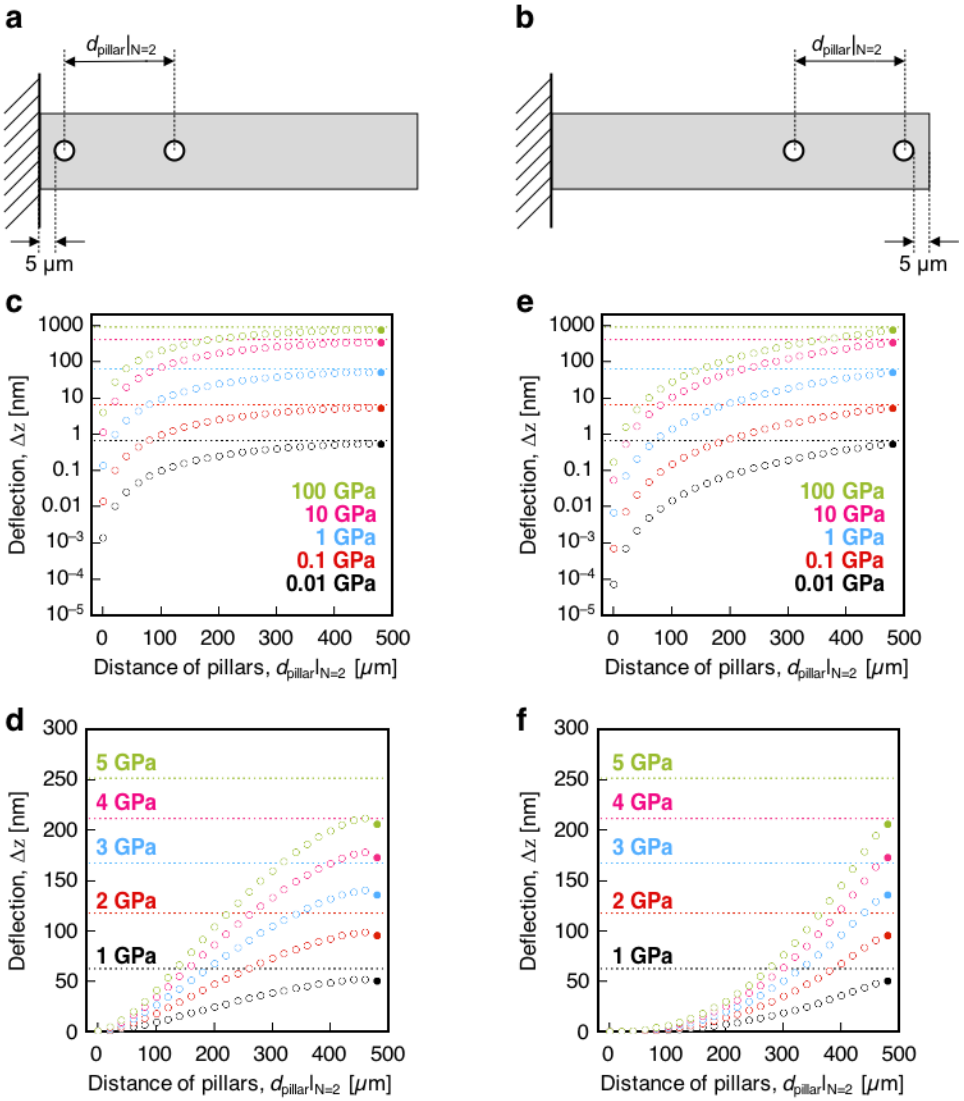

Fig. S5. Dependence of the deflection, Δ*z* on the distance between 2 pillars, $d_{pillar}|_{N=2}$ calculated by FEA. (a,b) Configuration of distance-dependent center aligned model with 2 pillars ($N = 2$). One of the pillars are placed at the fixed end (a) and at the free end (b), respectively, and the other pillar is varied at the center of cantilever plate with the distance, $d_{pillar}|_{N=2}$ [μm]. (c–f) The Young's modulus-dependent deflections, Δ*z* calculated by FEA as a function of $d_{pillar}|_{N=2}$ ranging from 20 μm to 480 μm for the fixed end (c–d) and the free end (e–f), respectively. The Young's moduli, E_f are varied from 0.01 GPa to 100 GPa (c,e) and from 1 GPa to 5 GPa (d,f). Dashed lines indicate the level of the deflections of the fully attached models. Solid and open circles are the center aligned model with $N = 2$ and the distance-dependent 2 pillars model, respectively.

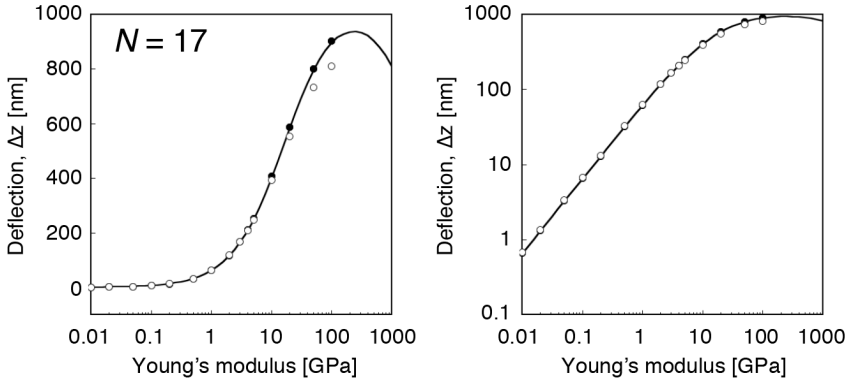

Fig. S6. Comparison between numerical and analytical solutions with number of pillars, $N = 17$. Results of the FEA simulations for center aligned model with number of pillars, $N = 17$ (distance between neighboring pillars is 30.5 μm.). The scales of y-axis are shown in linear (*left*) and logarithmic (*right*).

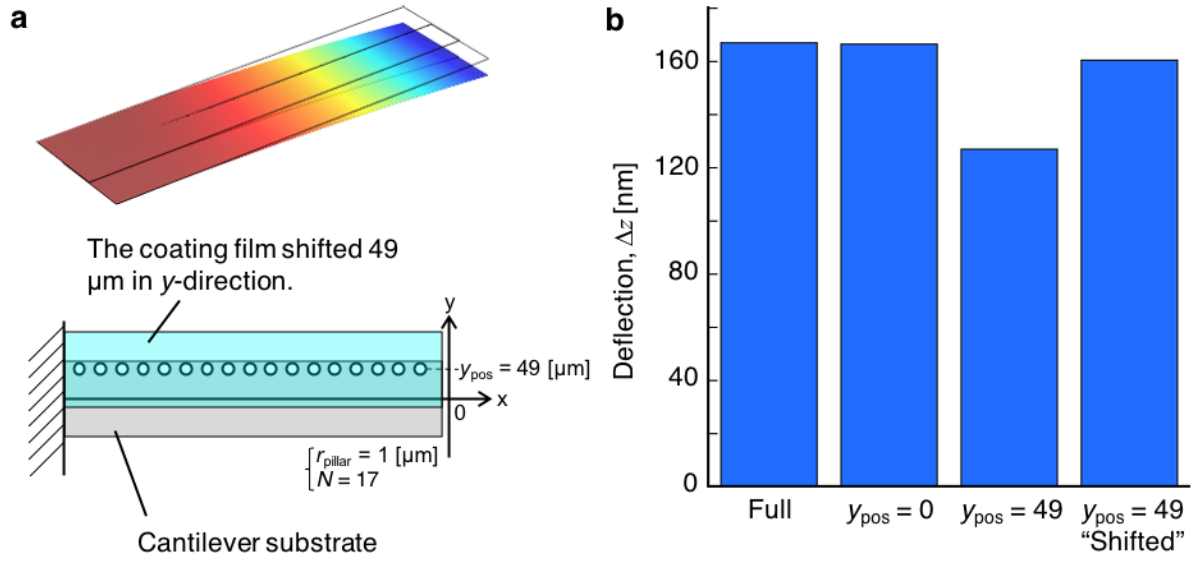

Fig. S7. Comparison between position of pillars and "shifted" model. (a) Configuration of "shifted" model. The coating film is shifted 49 nm in *y*-direction with 17 pillars at $y_{pos.}$ = 49 [μm]. The result of FEA (*top*) shows the Young's modulus of coating film, E_f at 3 GPa. (b) Comparison between the edge and shifted models. The deflections at the center of free end of cantilever, Δz are shown. The Young's modulus and Poisson's ratio of the coating film are 3 GPa and 0, respectively.

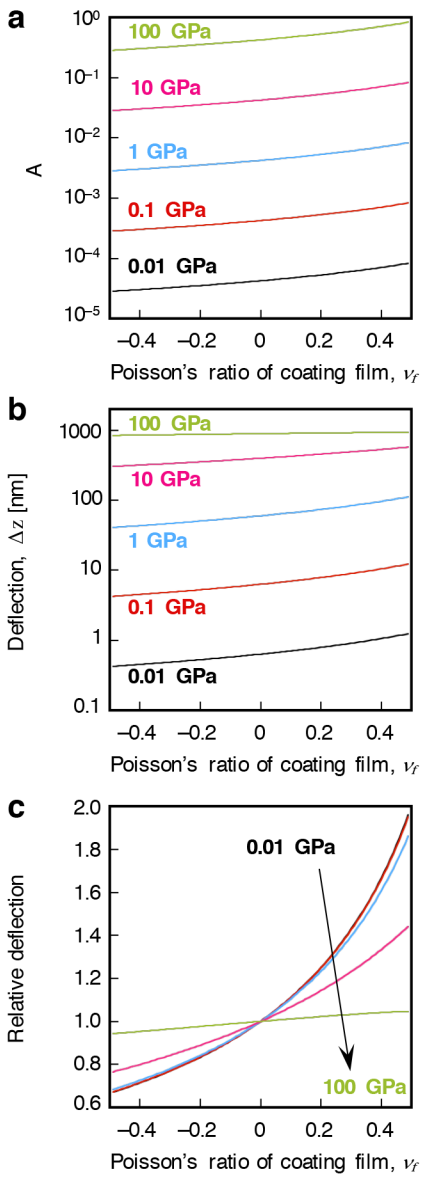

$$A = \frac{E_f w_f t_f}{1-\nu_f} \Big/ \frac{E_s w_s t_s}{1-\nu_s}$$

$$\Delta z = \frac{3l^2(t_f + t_s)}{(A+4)t_f^2 + (A^{-1}+4)t_s^2 + 6t_f t_s}\varepsilon_f$$

$$\frac{\Delta z}{\Delta z|_{\nu_f=0}}$$

Fig. S8. Poisson's ratio-dependent analytical solutions. (a) Poisson's ratio-dependent Eq. (3) in main text. (b) Poisson's ratio dependent deflection calculated by Eq. (2) in main text. (c) The relative deflection.

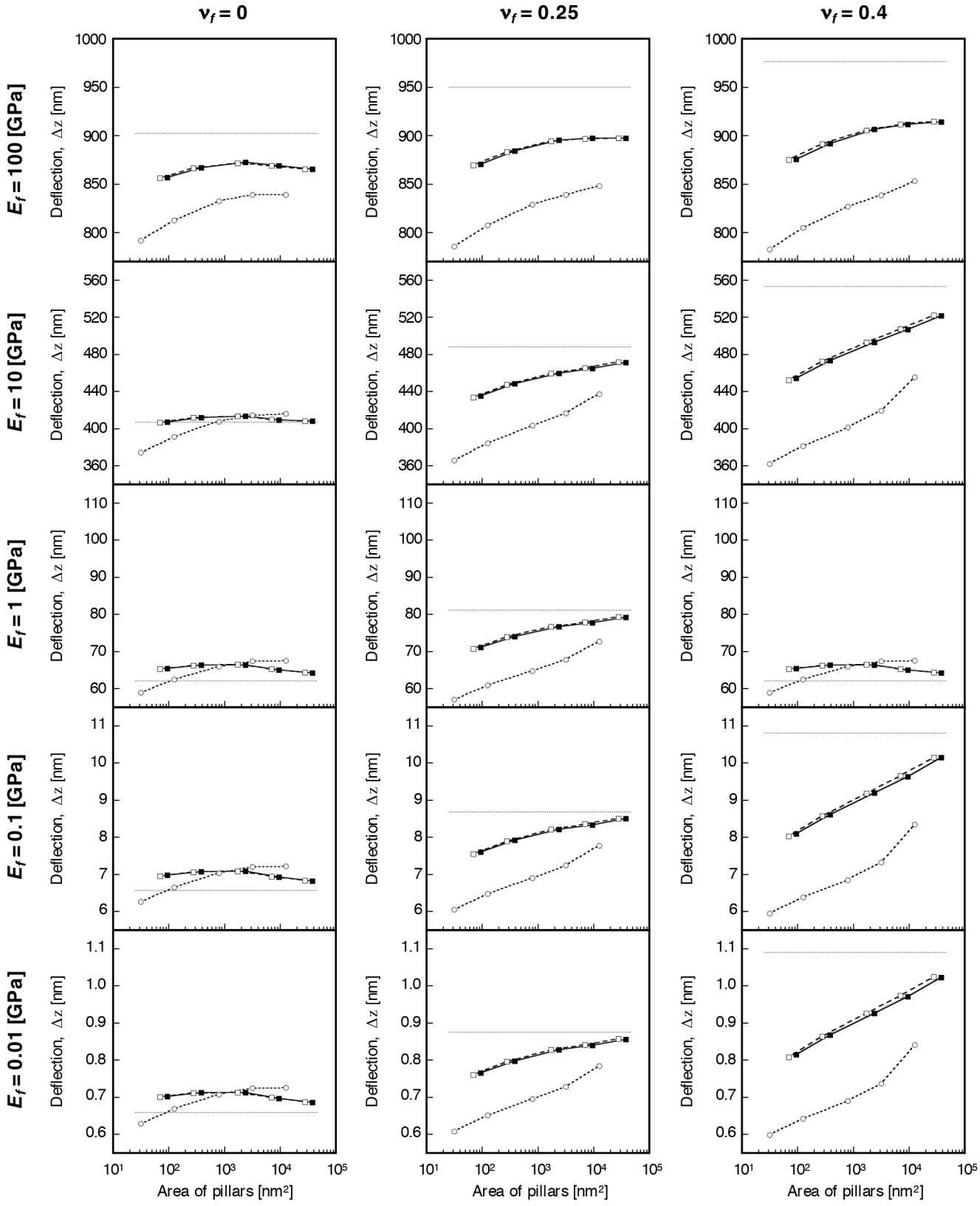

Fig. S9. Detailed effects of Poisson's ratio for three different interfacial attachment models, as presented in Fig. 2c in the main text. Young's modulus-dependent deflections, Δz, as a function of the area of the pillars. The Young's moduli, E_f, are varied from 0.01 to 100 GPa (see also Fig. S10 for the range of the Young's moduli from 1 to 5 GPa). Solid squares, open squares, and open circles are the uniformly distributed, peripheral distributed, and center aligned models, respectively. All dotted lines are the level of deflection of the conventional fully attached models.

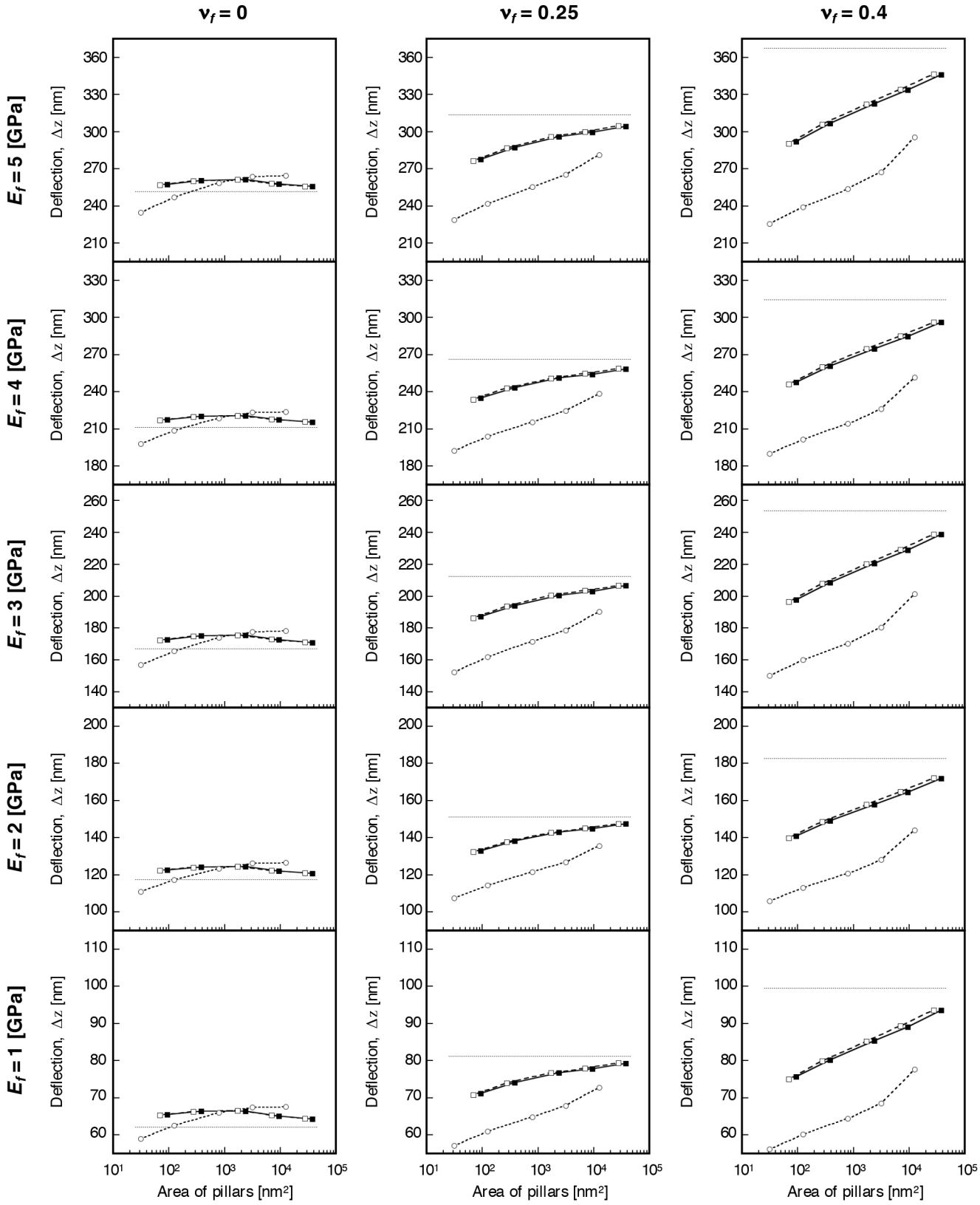

Fig. S10. Detailed effects of Poisson's ratio for three different interfacial attachment models, as presented in Fig. 2d in the main text. Young's modulus-dependent deflections, Δz, as a function of the area of the pillars. The Young's moduli, E_f, are varied from 1 to 5 GPa (see also Fig. S10 for the range of the Young's moduli from 0.01 to 100 GPa). Solid squares, open squares, and open circles are the uniformly distributed, peripheral distributed, and center aligned models, respectively. All dotted lines are the level of deflection of the conventional fully attached models.

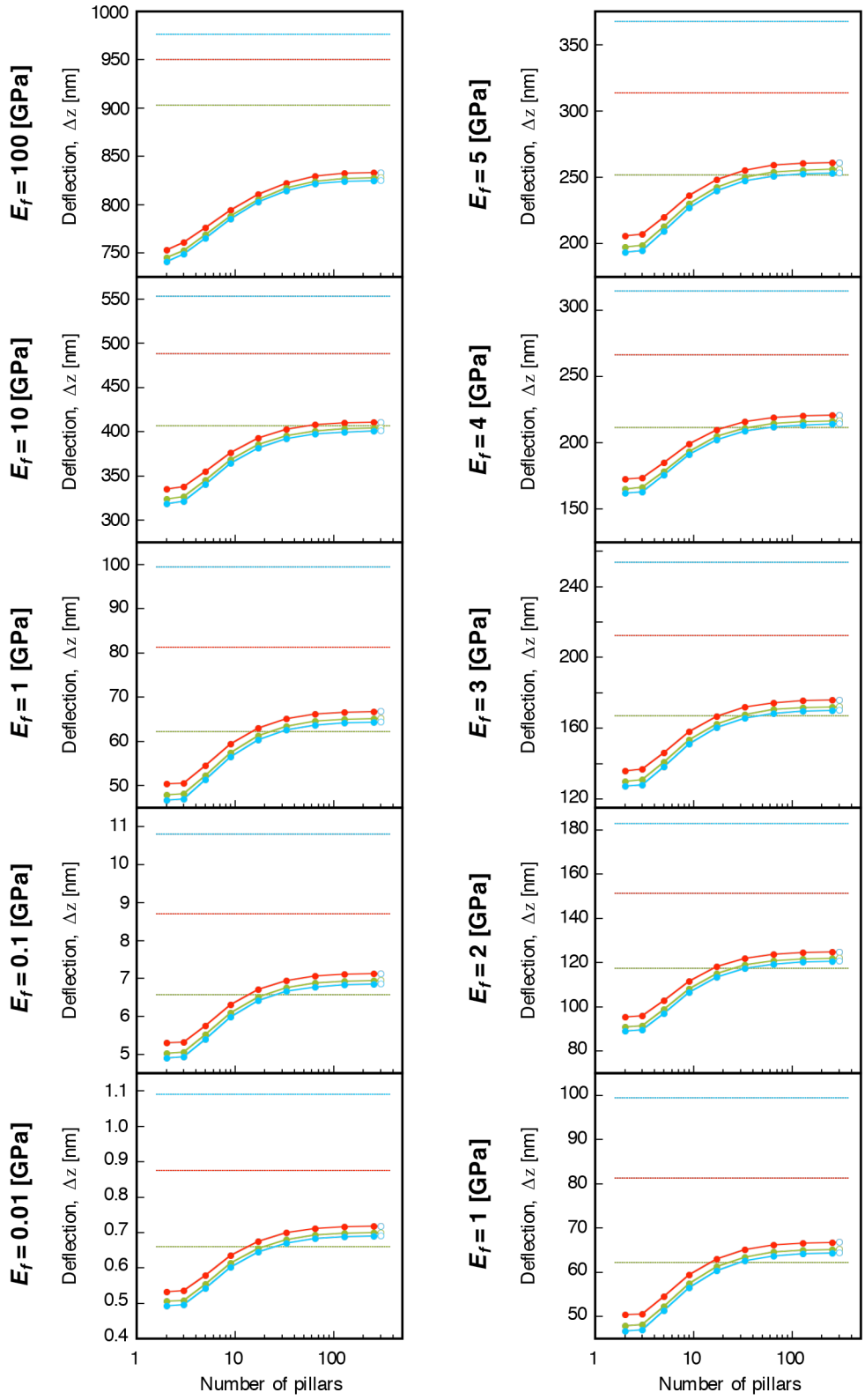

Fig. S11. Detailed effects of Poisson's ratio for the dependence of deflection, Δz, on the number of pillars calculated by FEA, as presented in Fig. 3b–c in the main text. The configuration of the number-dependent center aligned model is shown in Fig. 3a in the main text. The Young's modulus-dependent deflection, Δz, calculated by FEA as a function of the number of the pillars. The Young's moduli, E_f, are varied from 0.01 to 100 GPa (*left column*) and from 1 to 5 GPa (*right column*). Green, red, and light blue indicate the Poisson's ratio of coating film, ν_f, 0, 0.25, and 0.4, respectively. All dotted lines are the level of deflection of the conventional fully attached models.

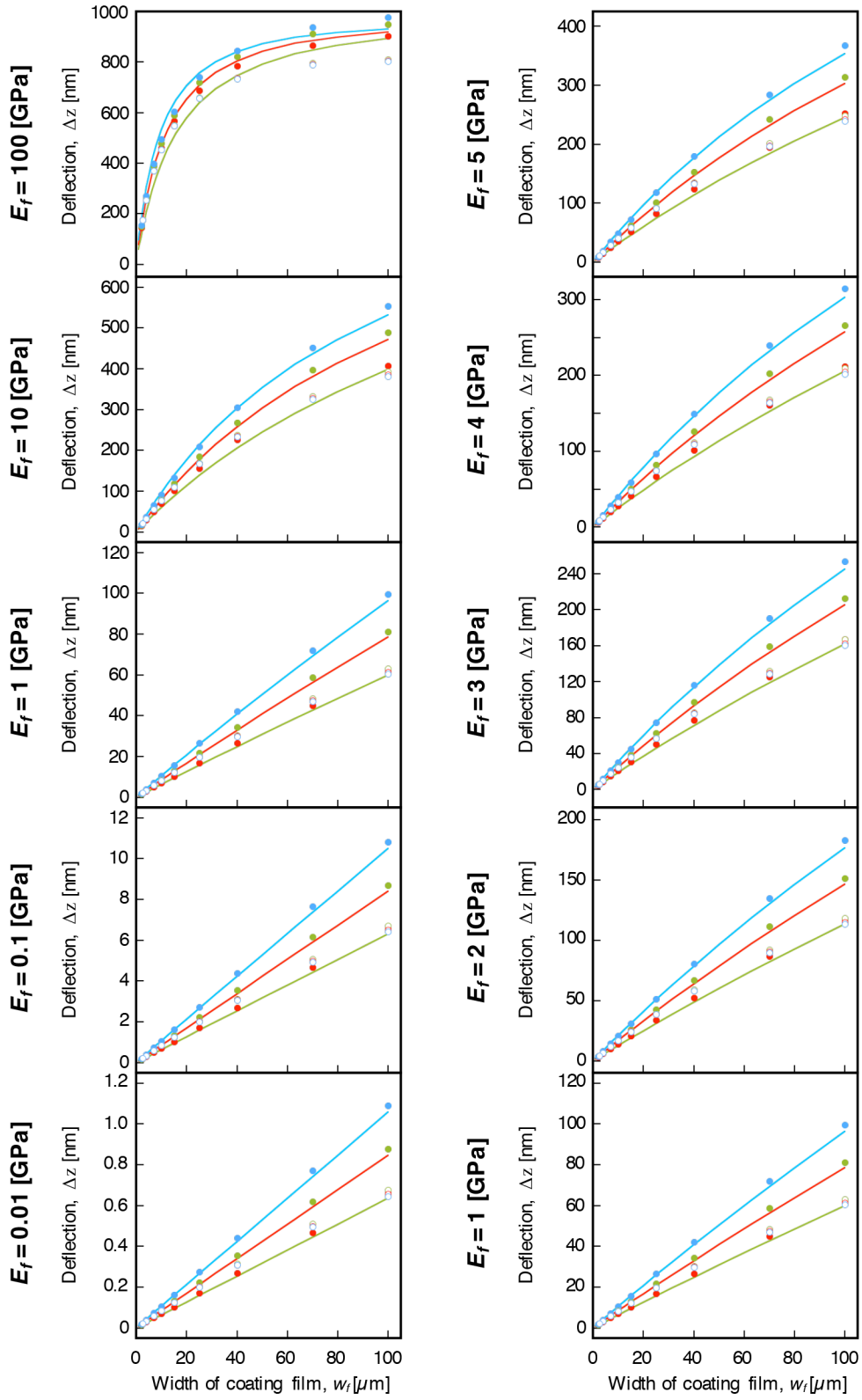

Fig. S12. Detailed effects of Poisson's ratio for the dependence of deflection, Δz, on the width of the coating films calculated by FEA, as presented in Fig. 5 in the main text. The configurations of the width-dependent models are shown in Fig. 5a in the main text. Solid lines are the results of the analytical model. Solid and open circles indicate the full attachment models and the center aligned models, respectively. The Young's moduli, E_f, are varied from 0.01 to 100 GPa (*left column*) and from 1 to 5 GPa (*right column*). Green, red, and light blue indicate the Poisson's ratio of coating film, ν_f, 0, 0.25, and 0.4, respectively. All dotted lines are the level of deflection of the conventional fully attached models.

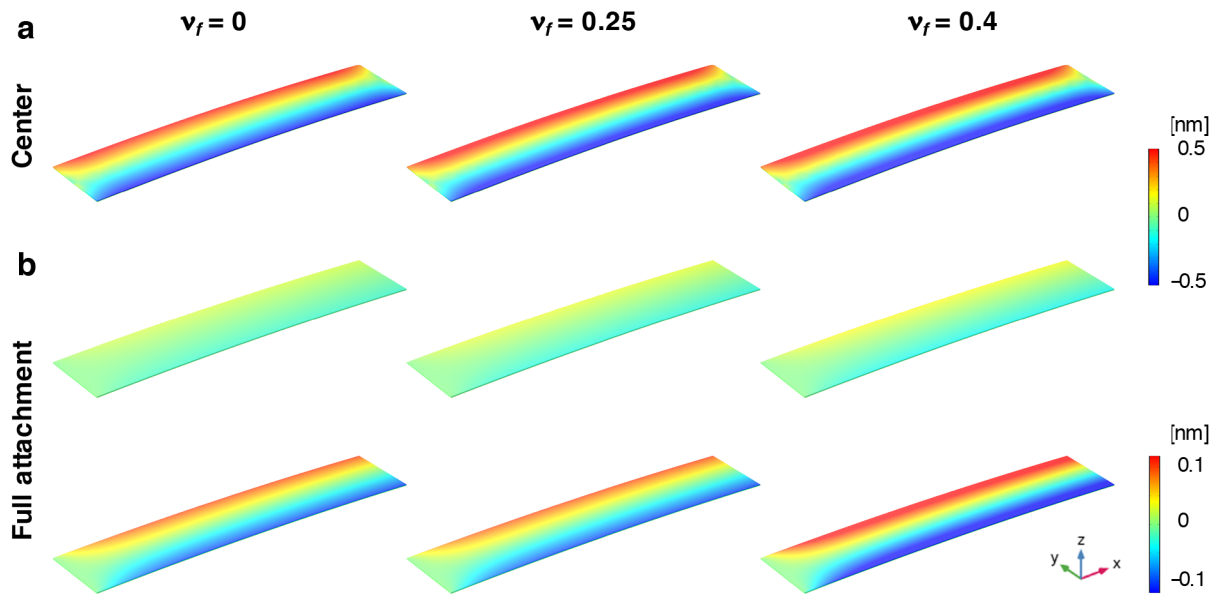

Fig. S13. The *y*-directional expansions of center aligned, and fully attached models calculated by FEA. (a) Results of the FEA simulations of the center aligned models with different Poisson's ratio of coating films in 3D view. The displacements in the *y*-direction are plotted as a color gradient ranging from –0.5 to 0.5 nm. (b) Results of the FEA simulations of the fully attached models with different Poisson's ratio of coating films. The displacements in the *y*-direction are plotted as a color gradient ranging from –0.5 to 0.5 nm (*top*) and from –0.12 to 0.12 nm (*bottom*), respectively. The Young's modulus, E_f, and the radius of pillars, r_{pillar}, shown in this figure are at 3 GPa and 5 μm, respectively.

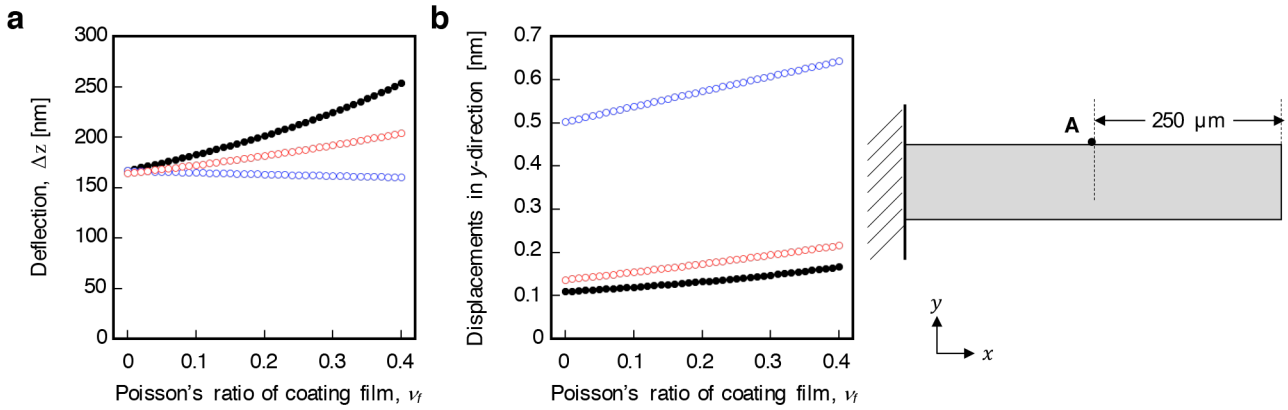

Fig. S14. Poisson's ratio-dependent deflection and displacements in *y*-direction calculated by FEA. (a) Poisson's ratio-dependent deflection, Δz, of fully attached models (black), center aligned models ($N = 17$) (blue), and uniformly distributed models ($N = 17 \times 3$) (red). (b) Poisson's ratio-dependent displacements in *y*-direction measured at the position A.

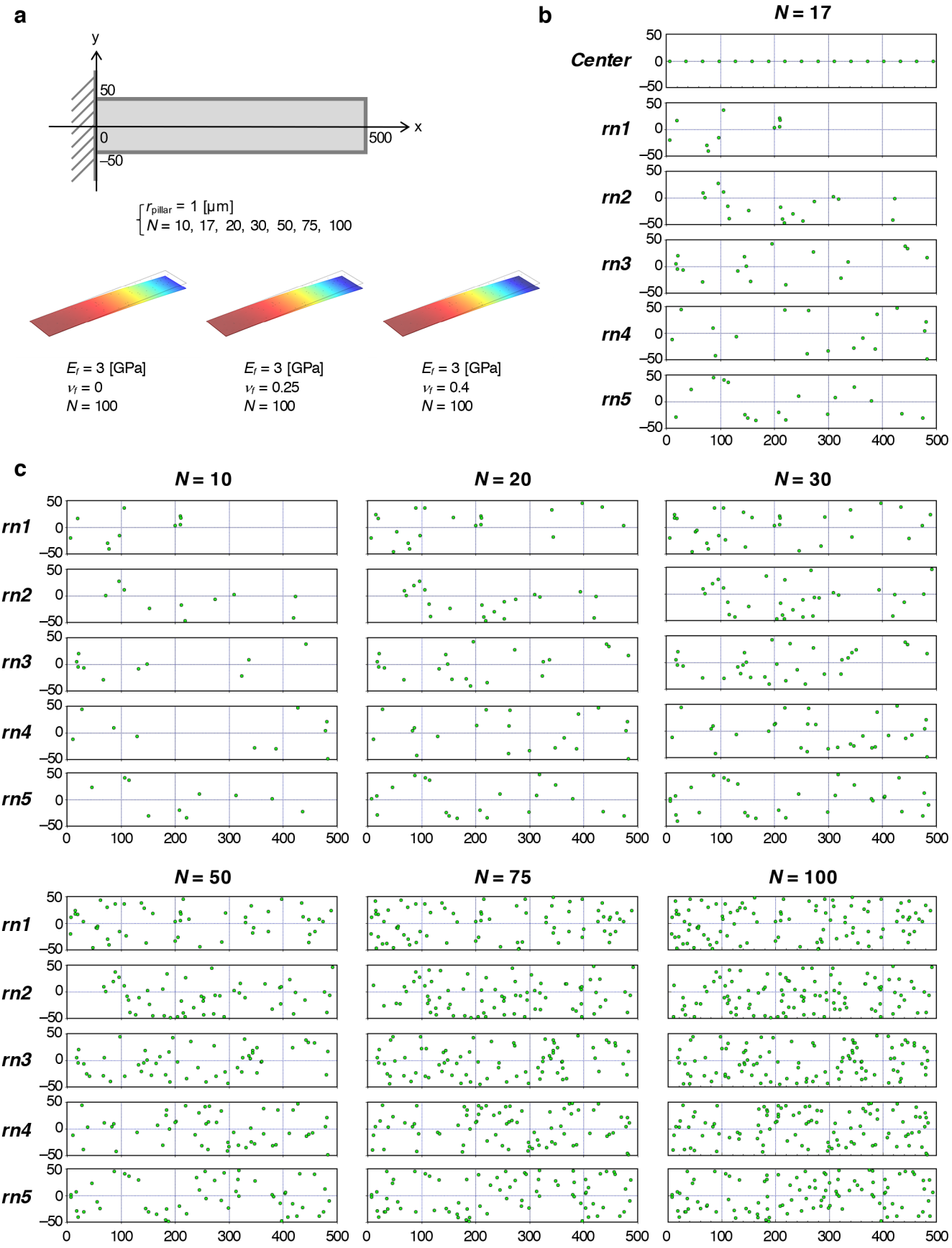

Fig. S15. Detailed configuration of randomly distributed models. (a) Configuration of a cantilever plate and an FEA simulation of randomly distributed model ($N = 100$, *rn1*) in 3D view. The displacements in the z-direction, Δz, are plotted as a color gradient ranging from 0 to 870 nm. (b) Comparison of pillar-distributions between center aligned model and randomly distributed models. Number of pillars, $N = 17$ is shown. (c) Randomly distributed models. All random numbers (*rn1*–*rn5*) are generated by Python (see also Supplementary Notes and Tables S3 and S4). Number of pillars, $N = 10$, 17, 20, 30, 50, 75.

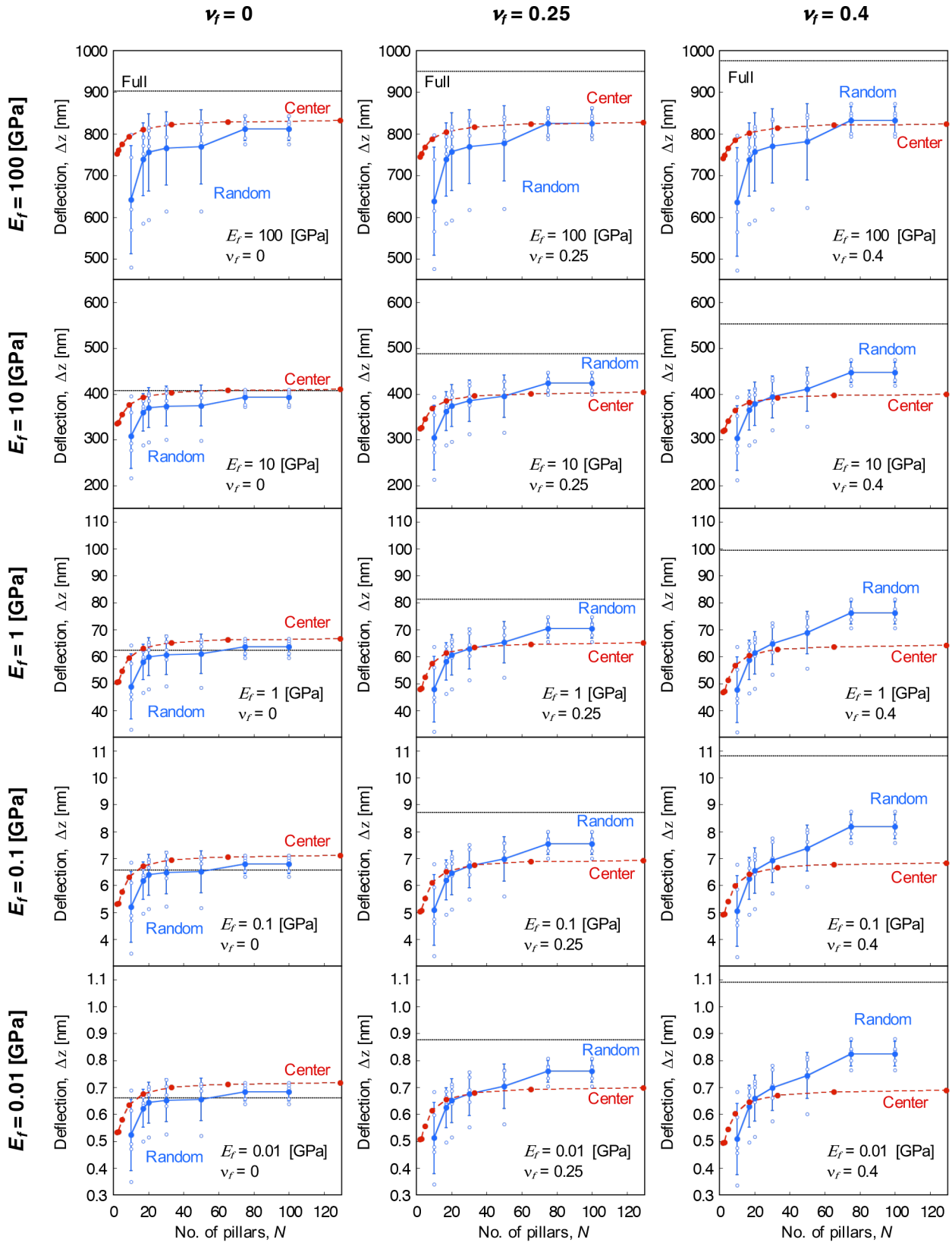

Fig. S16. Detailed effects of Poisson's ratio for randomly distributed models, as presented in Fig. 7 in the main text. Young's modulus-dependent deflections, Δz, as a function of the area of the pillars. The Young's moduli, E_f, are varied from 0.01 to 100 GPa (see also Fig. S17 for the range of the Young's moduli from 1 to 5 GPa). Blue open circles are the randomly distributed models with each series of the random number (*rn1*–*rn5*). Blue and red solid circles are the randomly distributed models, center aligned models, respectively. All dotted lines are the level of deflection of the conventional fully attached models.

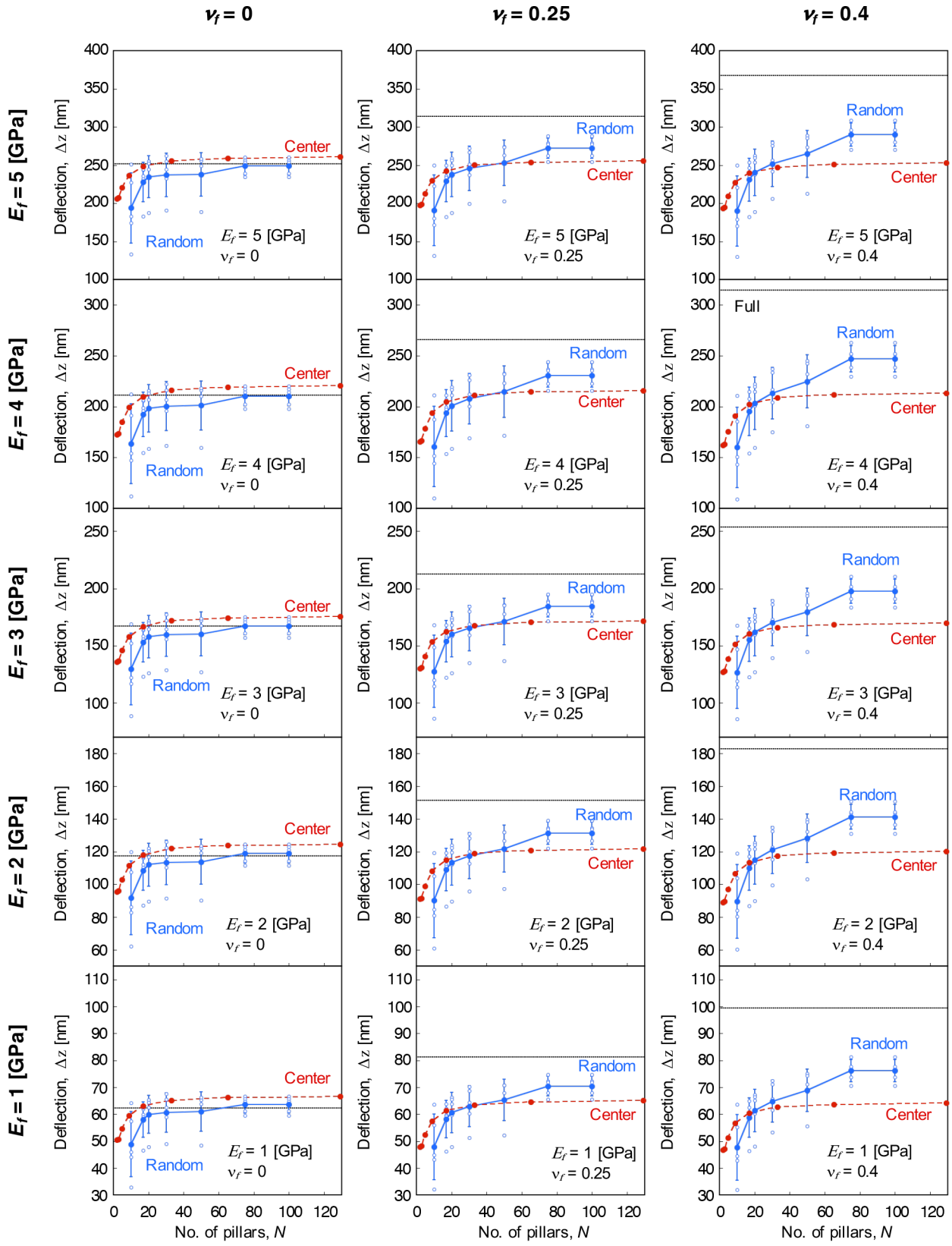

Fig. S17. Detailed effects of Poisson's ratio for randomly distributed models, as presented in Fig. 7 in the main text. Young's modulus-dependent deflections, Δz, as a function of the area of the pillars. The Young's moduli, E_f, are varied from 1 to 5 GPa (see also Fig. S16 for the range of the Young's moduli from 0.01 to 100 GPa). Blue open circles are the randomly distributed models with each series of the random number (*rn1*–*rn5*). Blue and red solid circles are the randomly distributed models, center aligned models, respectively. All dotted lines are the level of deflection of the conventional fully attached models.

Supplementary Tables

Table S1. Detailed parameters of uniformly distributed, peripheral distributed and center aligned models.

Model	No. of pillars, N	Radius of pillars, r_{pillar} [μm]	d_{pillar} [a,b] [μm]	d^0_{pillar} [b,c] [μm]	Area of pillars [μm^2]
Uniform	30	1	50	69	94.2
	30	2	50	68	376
	30	5	50	65	2360
	30	10	50	60	9420
	30	20	50	50	37700
Peripheral	22	1	50	69	69.1
	22	2	50	68	276
	22	5	50	65	1730
	22	10	50	60	6910
	22	20	50	50	27600
Center	10	1	50	69	31.4
	10	2	50	68	126
	10	5	50	65	785
	10	10	50	60	3140
	10	20	50	50	12600

[a] Center-to-center distance of neighboring pillars. See also Fig. S1.
[b] Values in parentheses are the shortest distance between the neighboring pillars ($d_{pillar} - 2 \times r_{pillar}$)
[c] Center-to-center distance from end of pillars to a neighboring pillar. See also Fig. S1.

Table S2. Detailed parameters of distance-dependent center aligned models.

No. of pillars, N	Radius of pillars, r_{pillar} [μm]	d_{pillar} [a,b] [μm]	Area of pillars [μm^2]
2	1	488 (486)	6.28
3	1	244 (242)	9.42
5	1	122 (120)	15.7
9	1	61.0 (59.0)	28.3
17	1	30.5 (28.5)	53.4
33	1	15.3 (13.3)	103
65	1	7.63 (5.63)	204
129	1	3.81 (1.81)	405
257	1	1.91 (–0.09)	807
Connected	1	0	979

[a] Center-to-center distance of neighboring pillars.
[b] Values in parentheses are the shortest distance between the neighboring pillars ($d_{pillar} - 2 \times r_{pillar}$)

Table S3. Detailed parameters of generated random numbers.

Entry	*rn1*		*rn2*		*rn3*		*rn4*		*rn5*	
	rn1(x)	*rn1(y)*	*rn2(x)*	*rn2(y)*	*rn3(x)*	*rn3(y)*	*rn4(x)*	*rn4(y)*	*rn5(x)*	*rn5(y)*
1	0.4170	0.7203	0.4360	0.0259	0.5508	0.7081	0.9670	0.5472	0.2220	0.8707
2	0.0001	0.3023	0.5497	0.4353	0.2909	0.5108	0.9727	0.7148	0.2067	0.9186
3	0.1468	0.0923	0.4204	0.3303	0.8929	0.8963	0.6977	0.2161	0.4884	0.6117
4	0.1863	0.3456	0.2046	0.6193	0.1256	0.2072	0.9763	0.0062	0.7659	0.5184
5	0.3968	0.5388	0.2997	0.2668	0.0515	0.4408	0.2530	0.4348	0.2968	0.1877
6	0.4192	0.6852	0.6211	0.5291	0.0299	0.4568	0.7794	0.1977	0.0807	0.7384
7	0.2045	0.8781	0.1346	0.5136	0.6491	0.2785	0.8630	0.9834	0.4413	0.1583
8	0.0274	0.6705	0.1844	0.7853	0.6763	0.5909	0.1638	0.5973	0.8799	0.2741
9	0.4173	0.5587	0.8540	0.4942	0.0240	0.5589	0.0090	0.3866	0.4142	0.2961
10	0.1404	0.1981	0.8466	0.0796	0.2593	0.4151	0.0442	0.9567	0.6288	0.5798
11	0.8007	0.9683	0.5052	0.0653	0.2835	0.6931	0.4361	0.9490	0.5999	0.2658
12	0.3134	0.6923	0.4281	0.0965	0.4405	0.1569	0.7863	0.8663	0.2847	0.2536
13	0.8764	0.8946	0.1272	0.5967	0.5446	0.7803	0.1732	0.0749	0.3276	0.1442
14	0.0850	0.0391	0.2260	0.1069	0.3064	0.2220	0.6007	0.1680	0.1656	0.9639
15	0.1698	0.8781	0.2203	0.3498	0.3880	0.9364	0.7334	0.4084	0.9602	0.1884
16	0.0983	0.4211	0.4678	0.2017	0.9760	0.6724	0.5279	0.9376	0.0243	0.2046
17	0.9579	0.5332	0.6404	0.4831	0.9028	0.8458	0.5217	0.1082	0.6998	0.7795
18	0.6919	0.3155	0.5052	0.3869	0.3780	0.0922	0.1582	0.5452	0.0229	0.5777
19	0.6865	0.8346	0.7936	0.5800	0.6534	0.5578	0.5244	0.6376	0.0016	0.5155
20	0.0183	0.7501	0.1623	0.7008	0.3616	0.2251	0.4015	0.6498	0.6398	0.9856
21	0.9889	0.7482	0.9646	0.5000	0.4065	0.4689	0.3969	0.6239	0.2591	0.8025
22	0.2804	0.7893	0.8895	0.3416	0.2692	0.2918	0.7674	0.1790	0.8705	0.9227
23	0.1032	0.4479	0.5671	0.4275	0.4577	0.8605	0.3756	0.5025	0.0022	0.4695
24	0.9086	0.2936	0.4367	0.7766	0.5863	0.2835	0.6867	0.2537	0.9815	0.3989
25	0.2878	0.1300	0.5356	0.9537	0.2780	0.4546	0.5547	0.6249	0.8137	0.5465
26	0.0194	0.6788	0.5442	0.0821	0.2054	0.2014	0.8955	0.3629	0.7709	0.4849
27	0.2116	0.2655	0.3663	0.8509	0.5140	0.0872	0.6376	0.1914	0.0291	0.0865
28	0.4916	0.0534	0.4063	0.0272	0.4836	0.3622	0.4978	0.1824	0.1115	0.2512
29	0.5741	0.1467	0.2472	0.0671	0.7077	0.7467	0.9184	0.4318	0.9649	0.6318
30	0.5893	0.6998	0.9939	0.9706	0.6911	0.6892	0.8302	0.4168	0.8167	0.5661
31	0.1023	0.4141	0.8003	0.6018	0.3736	0.6681	0.9047	0.4048	0.6354	0.8119
32	0.6944	0.4142	0.7650	0.1692	0.3398	0.5728	0.3312	0.5721	0.9267	0.9126
33	0.0500	0.5359	0.2930	0.5241	0.3258	0.4451	0.8454	0.8610	0.8248	0.0942
34	0.6638	0.5149	0.3566	0.0457	0.0615	0.2427	0.5957	0.0847	0.3610	0.0355
35	0.9446	0.5866	0.9832	0.4414	0.9716	0.2306	0.5973	0.2455	0.5464	0.7961
36	0.9034	0.1375	0.5040	0.3235	0.6915	0.6505	0.7326	0.8947	0.0511	0.1887
37	0.1393	0.8074	0.2597	0.3869	0.7239	0.4751	0.5147	0.6036	0.3655	0.2443
38	0.3977	0.1654	0.8320	0.7367	0.5967	0.0670	0.0651	0.5401	0.7951	0.3521
39	0.9275	0.3478	0.3792	0.0130	0.0726	0.1990	0.1292	0.6146	0.6389	0.4934
40	0.7508	0.7260	0.7974	0.2694	0.1519	0.1001	0.3637	0.7678	0.5835	0.9393
41	0.8833	0.6237	0.5827	0.0256	0.1293	0.5533	0.0485	0.1098	0.9435	0.1117
42	0.7509	0.3489	0.6622	0.3875	0.1878	0.9521	0.6840	0.5147	0.8436	0.3460
43	0.2699	0.8959	0.4971	0.4149	0.6816	0.5410	0.5716	0.8437	0.1008	0.3834
44	0.4281	0.9648	0.3509	0.5510	0.7072	0.2639	0.4877	0.8101	0.5104	0.9611
45	0.6634	0.6217	0.9729	0.1128	0.9267	0.8392	0.5102	0.9267	0.3715	0.0124
46	0.1147	0.9495	0.3133	0.0418	0.7263	0.4802	0.6669	0.1487	0.8597	0.1111
47	0.4499	0.5784	0.7384	0.6575	0.8421	0.7448	0.3646	0.8658	0.4783	0.8500
48	0.4081	0.2370	0.2146	0.4168	0.6603	0.9140	0.3503	0.1890	0.5147	0.4466
49	0.9034	0.5737	0.6438	0.6615	0.6337	0.3659	0.4726	0.3928	0.8005	0.0204
50	0.0029	0.6171	0.1705	0.8817	0.5528	0.1964	0.6189	0.4368	0.5726	0.4114

Table S3. Detailed parameters of generated random numbers. (*Continued*)

Entry	*rn1*		*rn2*		*rn3*		*rn4*		*rn5*	
	rn1(x)	*rn1(y)*	*rn2(x)*	*rn2(y)*	*rn3(x)*	*rn3(y)*	*rn4(x)*	*rn4(y)*	*rn5(x)*	*rn5(y)*
51	0.3266	0.5271	0.7780	0.1340	0.1921	0.7257	0.2609	0.4125	0.9851	0.8014
52	0.8859	0.3573	0.8689	0.7488	0.7849	0.9721	0.4190	0.9024	0.0540	0.1905
53	0.9085	0.6234	0.7986	0.5433	0.8510	0.5436	0.9796	0.6236	0.4524	0.7029
54	0.0158	0.9294	0.2208	0.9185	0.0898	0.4889	0.0832	0.7330	0.3320	0.3600
55	0.6909	0.9973	0.5921	0.3462	0.9279	0.7876	0.6787	0.8260	0.9215	0.9536
56	0.1723	0.1371	0.2638	0.9139	0.4851	0.4553	0.3475	0.0589	0.4077	0.8986
57	0.9326	0.6968	0.4197	0.5402	0.2180	0.1772	0.6118	0.1240	0.3303	0.0827
58	0.0660	0.7555	0.6084	0.8262	0.0736	0.8924	0.7595	0.7944	0.5267	0.6608
59	0.7539	0.9230	0.6236	0.1767	0.6402	0.1433	0.4086	0.9438	0.8930	0.9652
60	0.7115	0.1243	0.5913	0.4893	0.4141	0.0491	0.1738	0.9426	0.7699	0.7591
61	0.0199	0.0262	0.5479	0.6995	0.2094	0.7307	0.4655	0.7630	0.7100	0.7016
62	0.0283	0.2462	0.2458	0.1866	0.6511	0.4790	0.7528	0.9812	0.7673	0.9743
63	0.8600	0.5388	0.1106	0.2741	0.2748	0.6522	0.9733	0.0401	0.3737	0.0831
64	0.5528	0.8420	0.0103	0.6294	0.9564	0.4355	0.0160	0.5433	0.2396	0.2215
65	0.1242	0.2792	0.2952	0.1873	0.0701	0.0577	0.0339	0.6575	0.3636	0.8103
66	0.5858	0.9696	0.0953	0.2838	0.0829	0.9597	0.5349	0.6666	0.0601	0.4497
67	0.5610	0.0186	0.2149	0.2856	0.5408	0.8375	0.4413	0.2725	0.8132	0.2642
68	0.8006	0.2330	0.4714	0.5495	0.1700	0.2603	0.9497	0.7283	0.0634	0.2421
69	0.8071	0.3879	0.8451	0.9885	0.6920	0.8956	0.0063	0.0993	0.0851	0.8078
70	0.8635	0.7471	0.0489	0.2321	0.3407	0.0647	0.6317	0.2880	0.1703	0.1953
71	0.5562	0.1365	0.6433	0.1615	0.8641	0.2909	0.4076	0.7815	0.8146	0.8103
72	0.0599	0.1213	0.8701	0.2174	0.7411	0.1580	0.3541	0.9258	0.5894	0.9147
73	0.0446	0.1075	0.7418	0.6530	0.6950	0.8414	0.7205	0.5519	0.0598	0.9650
74	0.2257	0.7130	0.7989	0.0312	0.7272	0.3591	0.1810	0.4096	0.5710	0.3025
75	0.5597	0.0126	0.2296	0.7046	0.7267	0.1395	0.7629	0.9908	0.8257	0.6594
76	0.0720	0.9673	0.0876	0.0306	0.3138	0.4196	0.0737	0.1348	0.9865	0.1075
77	0.5681	0.2033	0.3571	0.5898	0.8772	0.1537	0.7400	0.8338	0.5809	0.4728
78	0.2523	0.7438	0.0522	0.0657	0.8801	0.7990	0.0888	0.8294	0.6523	0.2419
79	0.1954	0.5814	0.0435	0.3952	0.9716	0.3677	0.7867	0.6882	0.0311	0.5442
80	0.9700	0.8468	0.6684	0.1980	0.2049	0.2406	0.3399	0.4445	0.3647	0.8923
81	0.2398	0.4938	0.8763	0.4324	0.8279	0.9652	0.3663	0.8405	0.4593	0.4187
82	0.6200	0.8290	0.6196	0.2904	0.6988	0.4825	0.3283	0.3226	0.6329	0.5272
83	0.1568	0.0186	0.6153	0.9537	0.2870	0.8337	0.9353	0.9200	0.9612	0.7890
84	0.0700	0.4863	0.4480	0.2070	0.8722	0.0921	0.9687	0.8075	0.4967	0.2111
85	0.6063	0.5689	0.4254	0.4446	0.2159	0.8318	0.0869	0.0909	0.6040	0.7486
86	0.3174	0.9886	0.5076	0.5257	0.8483	0.3147	0.5571	0.8562	0.7559	0.9935
87	0.5797	0.3801	0.0424	0.1644	0.2793	0.4308	0.8842	0.6368	0.2185	0.4256
88	0.5509	0.7453	0.4502	0.7080	0.5394	0.0956	0.9558	0.1519	0.4238	0.3186
89	0.6692	0.2649	0.7776	0.7771	0.8369	0.5347	0.2216	0.3325	0.3653	0.4779
90	0.0663	0.3701	0.5028	0.9567	0.7750	0.2308	0.2568	0.3122	0.5421	0.2652
91	0.6297	0.2102	0.3319	0.4815	0.9653	0.7510	0.1184	0.3753	0.1344	0.3019
92	0.7528	0.0665	0.7484	0.8578	0.3431	0.9485	0.0298	0.5378	0.1365	0.3177
93	0.2603	0.8048	0.4145	0.8487	0.7005	0.8406	0.9458	0.4451	0.6792	0.6013
94	0.1934	0.6395	0.4446	0.7157	0.0455	0.0556	0.6242	0.6118	0.9972	0.5609
95	0.5247	0.9248	0.0084	0.0252	0.7427	0.3047	0.9334	0.7345	0.5487	0.6423
96	0.2633	0.0660	0.9405	0.1021	0.5168	0.1563	0.8248	0.3358	0.7268	0.6158
97	0.7351	0.7722	0.6620	0.2833	0.9780	0.5028	0.9075	0.1852	0.5885	0.6050
98	0.9078	0.9320	0.2008	0.3883	0.8290	0.0740	0.4080	0.7375	0.3548	0.7774
99	0.0140	0.2344	0.9259	0.5703	0.4789	0.0623	0.3335	0.8861	0.6046	0.3092
100	0.6168	0.9490	0.9167	0.7023	0.8842	0.4458	0.8607	0.1651	0.2456	0.0713

Table S4. Detailed parameters of randomly distributed models.

Entry	*rn1*		*rn2*		*rn3*		*rn4*		*rn5*	
	x	*y*	*x*	*y*	*x*	*y*	*x*	*y*	*x*	*y*
1	209.51	21.59	218.77	–46.46	21.59	20.40	477.91	4.63	114.33	36.33
2	6.06	–19.37	274.24	–6.34	147.96	1.06	480.67	21.05	106.88	41.02
3	77.62	–39.95	211.14	–16.63	441.76	38.84	346.49	–27.82	244.34	10.95
4	96.89	–15.14	105.87	11.69	67.29	–28.69	482.42	–48.39	379.76	1.80
5	199.62	3.80	152.23	–22.85	31.12	–5.80	129.46	–6.39	150.84	–30.60
6	210.57	18.15	309.11	2.86	20.58	–4.23	386.34	–29.63	45.40	23.37
7	105.77	37.06	71.68	1.33	322.78	–21.71	427.14	47.37	221.36	–33.49
8	19.37	16.71	96.01	27.96	336.01	8.90	85.96	9.54	435.41	–22.14
9	209.64	5.75	422.74	–0.56	17.70	5.77	10.39	–11.12	208.15	–19.98
10	74.51	–29.59	419.12	–41.19	132.52	–8.32	27.55	44.75	312.85	7.82
11	396.76	45.89	252.56	–42.60	144.36	18.93	218.84	44.00	298.77	–22.95
12	158.95	18.85	214.92	–39.54	220.94	–33.63	389.72	35.90	144.93	–24.15
13	433.68	38.67	68.05	9.48	271.79	27.47	90.50	–41.66	165.85	–34.87
14	47.50	–45.17	116.29	–38.52	155.51	–27.25	299.16	–32.54	86.82	45.47
15	88.88	37.06	113.51	–14.72	195.33	42.77	363.89	–8.97	474.59	–30.54
16	53.99	–7.73	234.28	–29.23	482.29	16.89	263.62	42.88	17.86	–28.95
17	473.45	3.25	318.52	–1.66	446.58	33.88	260.59	–38.40	347.52	27.39
18	343.64	–18.08	252.56	–11.08	190.46	–39.96	83.21	4.43	17.19	7.61
19	341.01	32.79	393.30	7.84	324.86	5.67	261.91	13.49	6.80	1.52
20	14.92	24.51	85.20	19.67	182.44	–26.94	201.93	14.68	318.22	47.59
21	488.56	24.32	476.70	0.00	204.38	–3.04	199.69	12.14	132.44	29.64
22	142.86	28.35	440.09	–15.52	137.39	–20.40	380.49	–31.46	430.80	41.43
23	56.37	–5.11	282.77	–7.10	229.35	35.33	189.28	0.25	7.08	–2.99
24	449.39	–20.23	219.13	27.10	292.09	–21.22	341.09	–24.14	484.96	–9.90
25	146.43	–36.26	267.37	44.47	141.65	–4.45	276.71	12.24	403.10	4.55
26	15.45	17.53	271.57	–40.95	106.24	–29.26	443.00	–13.44	382.18	–1.48
27	109.27	–22.98	184.78	34.38	256.85	–40.45	317.13	–30.24	20.21	–40.52
28	245.89	–43.77	204.26	–46.33	241.99	–13.51	248.92	–31.12	60.39	–24.38
29	286.17	–34.62	126.62	–42.42	351.35	24.18	454.17	–6.68	476.88	12.91
30	293.58	19.58	491.00	46.12	343.25	18.54	411.13	–8.16	404.53	6.48
31	55.94	–8.42	396.53	9.98	188.32	16.48	447.48	–9.33	316.05	30.57
32	344.87	–8.41	379.30	–32.42	171.85	7.13	167.61	7.07	458.22	40.44
33	30.38	3.52	149.00	2.36	164.99	–5.38	418.58	35.38	408.51	–39.77
34	329.93	1.46	180.03	–44.52	36.03	–25.22	296.70	–40.70	182.19	–45.52
35	466.96	8.48	485.78	–5.75	480.14	–26.40	297.47	–24.95	272.62	29.02
36	446.86	–35.53	251.95	–17.29	343.44	14.75	363.51	38.68	30.96	–30.51
37	73.97	30.12	132.76	–11.08	359.28	–2.44	257.19	10.15	184.35	–25.06
38	200.07	–32.80	412.02	23.20	297.17	–42.44	37.75	3.93	394.00	–14.49
39	458.62	–14.92	191.05	–47.72	41.41	–29.50	69.04	11.23	317.77	–0.65
40	372.40	22.15	395.13	–22.60	80.11	–39.19	183.46	26.24	290.75	43.05
41	437.05	12.12	290.35	–46.50	69.10	5.22	29.68	–38.24	466.45	–38.05
42	372.46	–14.81	329.15	–11.02	97.65	44.31	339.80	1.44	417.65	–15.09
43	137.72	38.80	248.57	–8.34	338.63	4.02	284.96	33.68	55.20	–11.43
44	214.91	45.55	177.23	5.00	351.10	–23.14	244.02	30.39	255.05	45.19
45	329.76	11.93	480.78	–37.95	458.24	33.24	255.00	41.82	187.30	–47.79
46	62.00	44.05	158.87	–44.90	360.44	–1.94	331.46	–34.42	425.54	–38.11
47	225.56	7.68	366.34	15.44	416.95	23.99	183.90	35.85	239.43	34.30
48	205.17	–25.77	110.74	–8.16	328.24	40.57	176.94	–30.48	257.19	–5.23
49	446.85	7.22	320.19	15.83	315.23	–13.14	236.64	–10.51	396.63	–47.00
50	7.40	11.48	89.19	37.40	275.79	–29.75	308.04	–6.20	285.44	–8.68

$x = rni(x) \times 488 + 6$ [μm] ($i = 1, \ldots, 5$)

$y = \{rni(y) - 0.5\} \times 98$ [μm] ($i = 1, \ldots, 5$)

Table S4. Detailed parameters of randomly distributed models. (*Continued*)

Entry	*rn1*		*rn2*		*rn3*		*rn4*		*rn5*	
	x	*y*	*x*	*y*	*x*	*y*	*x*	*y*	*x*	*y*
51	165.40	2.65	385.67	–35.87	99.73	22.12	133.33	–8.58	486.75	29.54
52	438.34	–13.99	430.03	24.38	389.05	46.27	210.49	39.44	32.33	–30.33
53	449.37	12.09	395.71	4.25	421.27	4.27	484.05	12.11	226.78	19.89
54	13.72	42.08	113.77	41.01	49.82	–1.09	46.59	22.83	168.04	–13.72
55	343.16	48.74	294.94	–15.07	458.83	28.19	337.20	31.95	455.68	44.46
56	90.10	–35.56	134.72	40.56	242.73	–4.38	175.56	–43.23	204.95	39.06
57	461.11	19.29	210.83	3.94	112.38	–31.63	304.57	–36.85	167.16	–40.89
58	38.21	25.04	302.92	31.97	41.93	38.45	376.65	28.85	263.04	15.76
59	373.89	41.46	310.30	–31.68	318.41	–34.95	205.41	43.49	441.78	45.59
60	353.22	–36.82	294.53	–1.05	208.09	–44.19	90.80	43.37	381.73	25.39
61	15.70	–46.43	273.38	19.55	108.17	22.61	233.16	25.77	352.50	19.75
62	19.81	–24.87	125.96	–30.71	323.75	–2.06	373.38	47.16	380.46	46.49
63	425.69	3.81	59.96	–22.14	140.09	14.92	480.96	–45.07	188.37	–40.86
64	275.78	33.52	11.00	12.68	472.75	–6.32	13.79	4.24	122.94	–27.29
65	66.60	–21.64	150.04	–30.65	40.22	–43.34	22.53	15.43	183.44	30.41
66	291.85	46.02	52.50	–21.19	46.44	45.05	267.03	16.32	35.33	–4.93
67	279.78	–47.17	110.88	–21.01	269.89	33.07	221.37	–22.30	402.83	–23.10
68	396.71	–26.17	236.05	4.85	88.98	–23.49	469.44	22.37	36.94	–25.27
69	399.87	–10.99	418.42	47.87	343.69	38.77	9.09	–39.27	47.51	30.16
70	427.41	24.22	29.85	–26.25	172.26	–42.66	314.27	–20.77	89.08	–29.86
71	277.45	–35.63	319.94	–33.18	427.69	–20.49	204.92	27.59	403.55	30.41
72	35.24	–37.11	430.63	–27.69	367.65	–33.51	178.82	41.73	293.61	40.64
73	27.74	–38.47	367.98	15.00	345.14	33.46	357.58	5.09	35.19	45.57
74	116.15	20.87	395.86	–45.94	360.85	–13.81	94.31	–8.86	284.64	–19.35
75	279.14	–47.77	118.03	20.05	360.62	–35.33	378.29	48.10	408.94	15.62
76	41.12	45.79	48.73	–46.00	159.14	–7.88	41.94	–35.79	487.41	–38.47
77	283.23	–29.08	180.28	8.80	434.08	–33.93	367.14	32.71	289.49	–2.66
78	129.13	23.89	31.48	–42.56	435.50	29.30	49.32	32.28	324.31	–25.30
79	101.37	7.97	27.23	–10.28	480.15	–12.97	389.93	18.45	21.19	4.33
80	479.37	33.99	332.19	–29.59	106.01	–25.42	171.88	–5.44	183.98	38.45
81	123.05	–0.61	433.62	–6.63	410.00	45.59	184.77	33.37	230.16	–7.97
82	308.54	32.24	308.39	–20.54	347.02	–1.72	166.22	–17.39	314.86	2.66
83	82.51	–47.18	306.24	44.46	146.08	32.70	462.42	41.16	475.07	28.32
84	40.17	–1.34	224.63	–28.71	431.62	–39.97	478.71	30.14	248.39	–28.31
85	301.89	6.75	213.58	–5.43	111.38	32.51	48.41	–40.09	300.74	24.36
86	160.87	47.88	253.72	2.52	419.97	–18.16	277.86	34.91	374.86	48.36
87	288.92	–11.75	26.71	–32.89	142.30	–6.78	437.49	13.41	112.63	–7.29
88	274.86	24.04	225.71	20.38	269.25	–39.63	472.43	–34.12	212.84	–17.77
89	332.59	–23.04	385.46	27.16	414.41	3.40	114.13	–16.42	184.28	–2.16
90	38.37	–12.73	251.36	44.76	384.18	–26.38	131.32	–18.40	270.54	–23.01
91	313.30	–28.40	167.95	–1.82	477.06	24.60	63.80	–12.22	71.57	–19.42
92	373.34	–42.48	371.21	35.07	173.43	43.96	20.53	3.70	72.60	–17.87
93	133.03	29.87	208.26	34.17	347.85	33.37	467.56	–5.38	337.44	9.93
94	100.40	13.67	222.95	21.14	28.20	–43.55	310.59	10.96	492.65	5.97
95	262.04	41.63	10.12	–46.53	368.46	–19.14	461.49	22.98	273.78	13.95
96	134.49	–42.54	464.94	–38.99	258.19	–33.69	408.51	–16.09	360.67	11.35
97	364.71	26.67	329.04	–21.24	483.24	0.27	448.84	–30.85	293.19	10.29
98	449.01	42.33	104.01	–10.94	410.55	–41.74	205.10	23.27	179.14	27.18
99	12.81	–26.03	457.84	6.89	239.71	–42.90	168.73	37.84	301.05	–18.70
100	306.99	44.00	453.36	19.82	437.51	–5.31	426.00	–32.82	125.87	–42.02